Alignment of Ethyl Halide Molecules (C_2H_5X, X= I, Br, Cl) Induced by Strong ps Laser Irradiation

S. Kaziannis, C. Kosmidis,* and A. Lyras

Department of Physics, University of Ioannina, 45110 Ioannina, Greece

Received: November 1, 2007; Revised Manuscript Received: March 7, 2008

The alignment of polyatomic molecules under strong 35 ps laser irradiation is investigated for a broad range of laser intensities (10^{13}–10^{15} W/cm^2) using time-of-flight mass spectrometry. The dynamic alignment of the molecules under study (C_2H_5X, X = I, Br, Cl) is verified in single-pulse experiments by recording the fragments' angular distributions, their dependence on the laser intensity, and also the comparison of the ionic signal of the various fragments recorded for linear and circular polarization. For all cases, the angular distributions of the Coulomb explosion fragments are found to be independent of the laser peak intensity, implying that the molecular alignment is taking place during the rise time of the laser pulses at relatively low intensities (10^{13} W/cm^2). Moreover, the same result implies that the alignment mechanism is close to the adiabatic limit, albeit the laser pulse duration is much shorter than the characteristic rotational times ($1/2B$) of the molecules under study. Finally, by comparing the angular distributions of the different molecules, we conclude that the degree of alignment is only weakly dependent on the molecular mass and the moment of inertia under the irradiation conditions applied.

Introduction

The alignment of molecules during their multielecton dissociative ionization induced by strong ps and fs laser pulses ($>10^{13}$ W/cm^2) has been the subject of numerous publications since the early 90s.[1,2] The major part of the literature concerns the interaction of relatively small molecules with strong laser fields. From the early published works, the main experimental observation related to the possible alignment of molecules during their interaction with strong laser fields was the ejection anisotropy of the produced fragment ions with respect to the laser polarization direction. For the case of diatomic molecules, it is usually found that the various atomic fragments are ejected along the laser polarization axis, with only few exceptions reported recently for molecular oxygen[3] and noble gas dimers.[4,5] For the case of triatomic molecules, the produced ions coming from the outer atoms are ejected parallel to the laser polarization, while the middle atomic ions are ejected parallel or perpendicular to the same axis, depending on the laser pulse duration.[6–9]

However, the reported anisotropy is by no means an unambiguous proof of the molecular alignment by the laser electric field and can alternatively be interpreted as a sign of the well-known geometric alignment mechanism, which, in fact, refers to the dependence of the ionization probability on the angle between the electric field and the molecular axis.[10] Different ways of disentangling the actual reorientation of the molecular axis toward the laser electric field (often referred to as dynamic alignment) from the geometric alignment effect have been proposed, for instance, the dependence of the angular distributions characteristics (fwhm, ratio of its maximum value to the minimum one) on the laser intensity[10–12] and the comparison of the ionic signal recorded with linearly and circularly polarized laser fields.[13] These methods are used in single-laser experiments where the same laser pulse is used for the molecular alignment and for the dissociative ionization of the molecular sample.

At the same time, the majority of publications over the last eight years, investigating the alignment mechanism report results from pump−probe experimental schemes. The pump beam is used for the alignment of the studied molecules, exclusively, while its intensity is lower than the ionization threshold. The probe beam is usually a laser pulse of short duration in order to achieve a good temporal resolution in the measurement of the molecular alignment. The degree of alignment can be inferred either by using a strong probe laser beam that photodissociates the aligned molecules and enables the recording of the produced fragments' angular distributions[14,15] or by using low-intensity probe beams and recording the alignment by optical methods.[16–18] Using the two-pulse experimental scheme, the alignment of neutral diatomic and polyatomic molecules can be achieved by using ns laser pulses at relatively low laser intensity ($\sim 10^{12}$ W/cm^2).[15,19] On the other hand, Rosca-Prunna et al. were the first to experimentally show that the alignment of neutral molecules was also achievable by pulses of subpicosecond duration for the case of heavy diatomic molecules, such as I_2 and Br_2.[20,21] These different approaches for molecular alignment, that is, the long- and short-pulse limit with respect to the molecular rotational period, are usually referred in the literature as "adiabatic" and "nonadiabatic" alignment, respectively, and they have been investigated extensively both experimentally and theoretically. For a complete overview of the corresponding literature, the reader is referred to review articles in refs 22 and 23, and the references therein, and recent reports.[24–29] In addition, for the case of asymmetric top polyatomic molecules, the reader is referred to refs30–34. Nevertheless, there are only a few publications concerning the intermediate region. To the best of our knowledge, Vrakking and co-workers[20,21] are the only group that has experimentally investigated the alignment mechanism for diatomic molecules interacting with laser pulses of 500 fs to 10 ps duration and the transition from the nonadiabatic to the adiabatic regimes. Moreover, there are few

* To whom correspondence should be addressed. E-mail: kkosmid@uoi.gr. Fax: +30-26510-98695.

10.1021/jp710540r CCC: $40.75
Published on Web 05/01/2008

theoretical investigations dealing with the transition between the two regimes.[35–37]

Therefore, we believe that there is a need for further experimental work on the molecular alignment by laser pulses of ps duration, which, in fact, lies in the intermediate region between the adiabatic and nonadiabatic regime, depending on the characteristic rotational times of the specific molecular system under investigation. Thus, in the present work, we investigate the alignment of asymmetric top molecules interacting with laser irradiation of 35 ps duration. Particularly, the duration of the laser pulse is about one-fifth to one-third of the characteristic rotational times (1/2*B*, where *B(*MHz*)* is the rotational constant) of the molecules under study (C_2H_5X, X = I, Br, Cl). The experiments were performed using a single laser beam, and in order to explore the dynamic or geometric alignment of the particular polyatomic molecules, the angular distributions of the ionic fragments have been recorded under various irradiation conditions. Finally, the ethyl halides have been selected for this study because their multielectron dissociative ionization (MEDI) processes have recently been explored by our research group,[38] as they offer the opportunity to study the influence of the molecular mass and moment of inertia on the efficiency of the alignment process.

Experimental Details

The Nd:YAG picosecond laser system (Quantel YG-901C) used produces 35 ps pulses at 1064 nm, with 80 mJ of energy per pulse at a repetition rate of 10 Hz.

A time-of-flight mass spectrometer based on a Wiley–McLaren design, with a 1.4 m long field-free tube, was used for ion analysis. The ions produced in the molecule−laser interaction region were accelerated by a dual stage electrostatic field under variable potential (0–3000 V). An electrode with a 1 mm pinhole separated the two field stages. Furthermore, in order to increase the angular and mass resolution of the spectrometer, another 1 mm pinhole at a distance of 12 cm from the acceleration region was added. The electronic signal was recorded with an Agilent 54830B (600 MHz, 4Gs/s) digital oscilloscope. The mass resolution was typically 700 at 100 Da.

The background pressure of the system was below 10^{-7} Torr, and the molecular vapor was allowed to expand through a needle valve into the interaction region. The experiments were performed while the pressure in the chamber was kept below 3×10^{-7} Torr in order to ensure that no space-charge effects were perturbing the mass spectrum measurements.

The studied alkyl halides were purchased from Fluka and had a purity of better than 99.5%, while they were used after several repeated freeze–thaw−degassing cycles under vacuum.

The laser light was focused with a 250 mm focal length lens at about 1 cm from the repeller electrode. Taking into account the Gaussian profile of the 1064 nm laser beam, the diameter of the beam at the focus is estimated to be 33 μm, while the corresponding Rayleigh range is estimated to be 3.2 mm, which is significantly longer than the width of the spectrometer's pinholes, mentioned above. Thus, the combination of the particular focal length lens and the small-diameter pinholes ensures that the ionic signal collected is generated only in the central portion of the total focal volume. The polarization of the laser light was controlled with a Brewster angle polarizer and was rotated by using a half-wavelength plate. The intensities attained at the focus were also checked through comparison with the intensities needed to produce multiply charged argon ions.[39]

Results and Discussion

The mass spectra of the studied ethyl halides are presented in Figure 1. They have been recorded at an intensity of 1.5×10^{14} W/cm^2, with the direction of the laser polarization parallel (solid line) and perpendicular (dash−dot line) to the TOF axis. The MEDI processes of these molecules, induced by moderately strong ps laser pulses, have been reported recently.[38] The ion peaks that correspond to the halogen ions and, in some cases, to the $[P-X]^+$ ions (where P stands for the parent molecule and X for the halogen atom) are found to consist of two pairs of components when the laser polarization is set parallel to the TOF axis. The outer pair of components is formed by high kinetic energy fragments (labeled as out), while the middle one (labeled as mid) is formed by those with low kinetic energy. On the basis of the angular distribution of the individual components of the aforementioned fragment ions, their dependence on laser intensity, and their kinetic energy values, different ionization/dissociation channels have been identified.

The outer components of the X^+_{out} and $[P-X]^+_{out}$ ion peaks were found to be produced mainly by the Coulomb explosion of doubly charged parent ions $[P^{2+}]$ that takes place when the C−X bond length reaches a critical value, which is about twice that of the equilibrium

$$[P^{2+}] \rightarrow [P-X]^+_{out} + X^+_{out} \quad (1)$$

The X^{2+}_{out} ions are attributed to the Coulomb explosion of higher charged parent ions, probably the $[P^{3+}]$, taking place at the same critical length of the elongated C−X bond

$$[P^{3+}] \rightarrow ([P-X]^+)^* + X^{2+}_{out} \quad (2)$$

The X^+_{mid} and X^{2+}_{mid} ions originate from neutral and/or ionic halogen atoms of low kinetic energy, liberated by the dissociation of the singly charged parent ions. The released halogen atoms are ionized by the same laser pulse, in sequential steps, to their final charge state. Obviously, a similar ionization mechanism could be also in operation for the X^+_{out} ions, resulting thus in the production of X^{2+}_{out} ions of relatively lower kinetic energy compared to that of the species generated from the Coulomb explosion of the triply charged $[P^{3+}]$ parent ions. Actually, as the laser intensity increases, the probability for multiply charged atomic ion production via sequential atomic ionization steps increases. The ejection of multiply charged atomic fragment ions through the dissociation of multiply charged parent ions is more probable at lower laser intensities (for instance, at $\sim 10^{14}$ W/cm^2).[38]

The discrimination of the various dissociating channels was possible for the ethyl bromide and ethyl chloride molecules. For the case of ethyl iodide, the angular distributions of the individual components could not be accurately recorded for the halogen ions, while this was possible for the molecular ionic fragments ($[P-X]^+$). Nevertheless, the ionization/dissociation mechanism for this compound was found to be similar to that proposed for the ethyl bromide and ethyl chloride molecules.

All of the ions mentioned above exhibit a single peak profile when the laser polarization is perpendicular to the TOF axis. This observation indicates that the C−X molecular bond is aligned with respect to the laser electric field prior to or during the dissociative ionization. This conclusion is also supported by the fact that the recorded angular distributions for the atomic and molecular ionic fragments present a maximum value when the laser polarization is parallel to the detection axis (TOF axis) and a minimum in the perpendicular direction, as depicted in Figures 2–4.

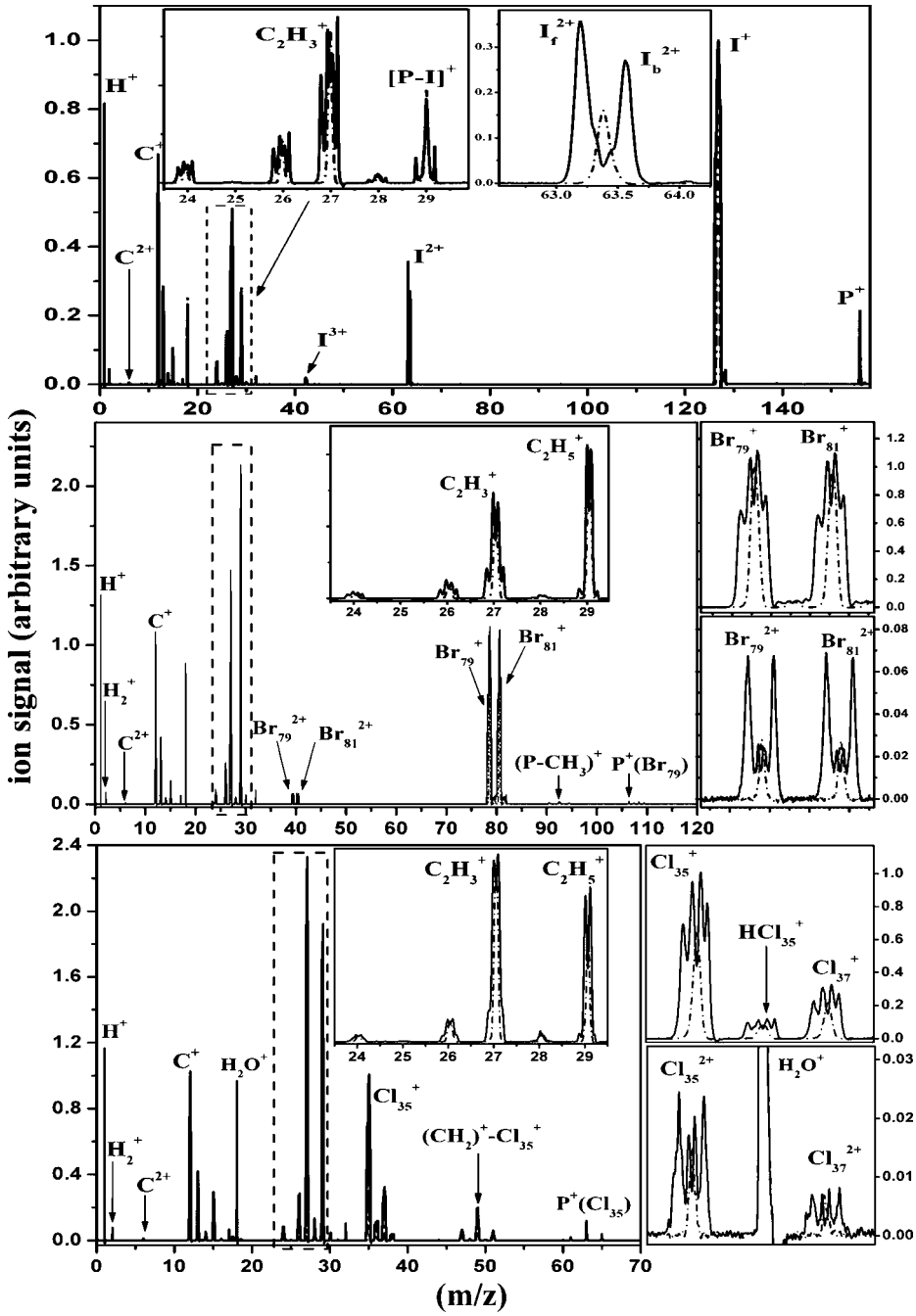

Figure 1. The mass spectra of ethyl iodides recorded at 1.5×10^{14} W/cm^2 with parallel (solid line) and perpendicular (dash−dot line) laser polarization with respect to the TOF axis.

However, these experimental findings are not a priori, implying the dynamic alignment of the molecules under study since the same results could be interpreted by the geometric alignment mechanism too; the laser electric field is not strong enough to ionize and photodissociate the molecules when the laser polarization is perpendicular to the C−X bond direction. This serves also as a plausible explanation for the absence of the X^+_{out}, $[P-X]^+_{out}$, and X^{2+}_{out} ions from the mass spectra recorded with perpendicular polarization. The generation of the corresponding molecular ions requires a strong coupling between the laser electric field and the C−X bond, which is the bond of maximum polarization for the ethyl halide molecules. Thus, for perpendicular laser polarization, the multiple molecular ionization leads to the production of high kinetic energy fragment ions, with their velocity vectors laying within a small angle with respect to the laser electric field, and they eventually miss the MCP detector. The same argument could also be applied for the interpretation of the single peak profile of the corresponding fragments produced by the dissociation of singly charged parent ions.

On the other hand, the single ionization rate is not expected to be strongly dependent on the angle between the C−X bond and laser polarization as it is for the multiple ionization rates. It is known that, even for the case of linear diatomic molecules, the ratio of the single ionization rate for parallel and perpendicular polarization with respect to the molecular bond is 4/1 and 2/1 for the N_2[40,41] and CO[42] molecules, respectively.

Thus, the single peak profiles of the X^+_{mid}, X^{2+}_{mid}, and $[P-X]^+_{mid}$ fragments recorded with perpendicular laser polarization imply the dynamic alignment of the molecules under study, taking place at the rise time of the laser pulse, before the laser electric field becomes strong enough to ionize and

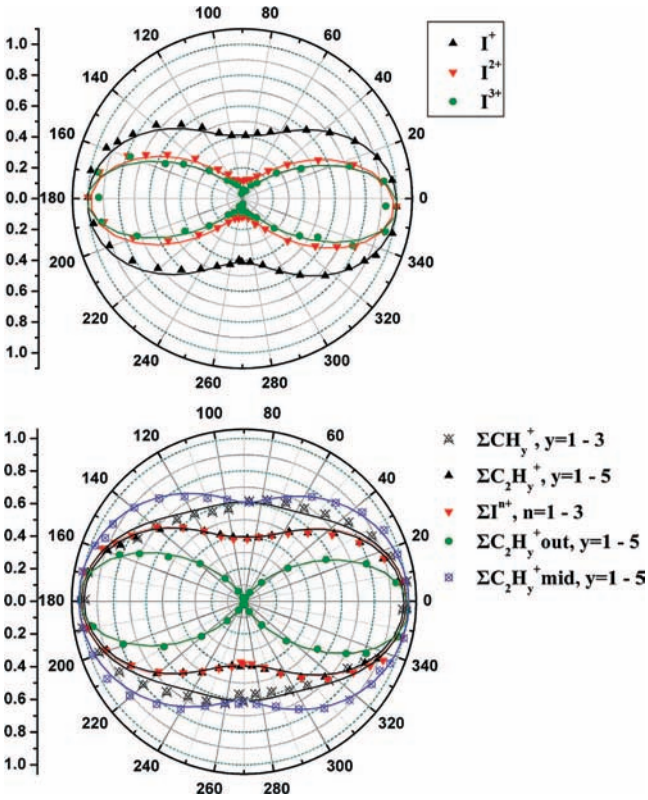

Figure 2. The angular distributions of the ethyl iodide fragment ions recorded at the intensity of 1.0×10^{14} W/cm^2.

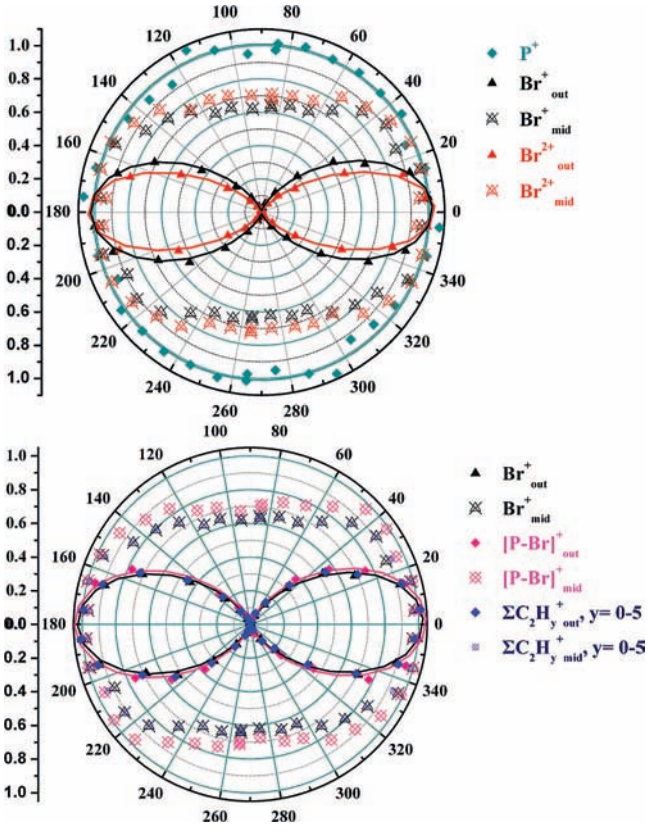

Figure 3. The angular distributions of the ethyl bromide fragment ions recorded at the intensity of 1.0×10^{14} W/cm^2. The data presented for the Br^+ and Br^{2+} distributions correspond to the Br_{81} isotope. The Br_{79} isotope exhibits the same angular distributions.

dissociate the molecules under study. In order to investigate the alignment mechanism, we have recorded the angular

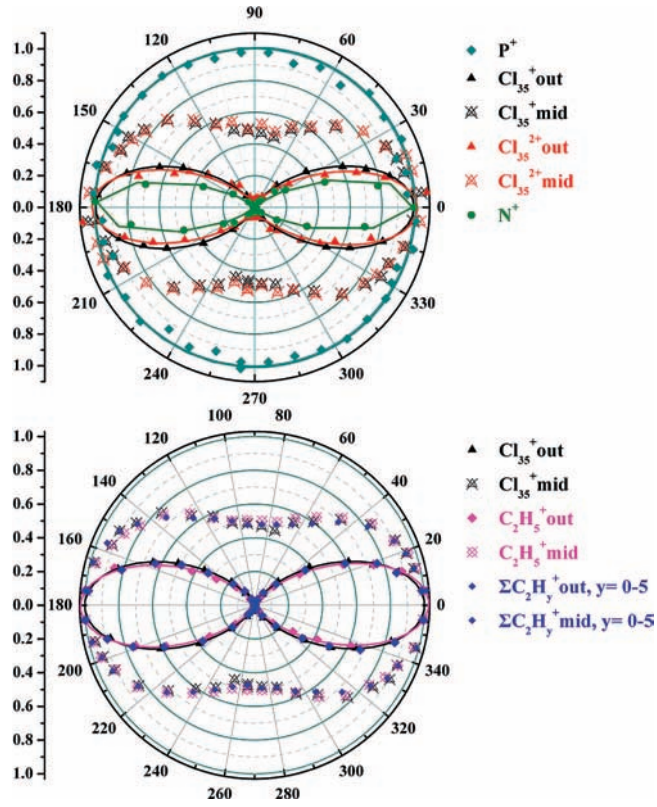

Figure 4. The angular distributions of the ethyl chloride fragment ions recorded at the intensity of 1.0×10^{14} W/cm^2. The data presented for the Cl^+ and Cl^{2+} distributions correspond to the Cl_{35} isotope. The Cl_{37} isotope exhibits the same angular distributions.

distributions for different laser intensities. The sharpness of the angular distributions is assessed by fitting the experimental data with the function $A + B \cdot \cos^n(\Theta)$ (see Figures 2–4), where A is the isotropic component, B is the anisotropic one, and n is the degree of alignment.[43]

As mentioned above, the discrimination of the various dissociation channels is not possible for the case of the C_2H_5I molecule, while the C_2H_5Cl and C_2H_5Br molecules exhibit similar dependence on the experimental parameters. For simplicity, we present the results in detail for the case of the C_2H_5Cl molecule, while the corresponding data for the rest of the ethyl halides will be compared to those of the ethyl chloride.

The Ethyl Chloride Case. In Figure 5, the degree of alignment (n) of the chloride ions as a function of the laser intensity is presented. The data acquired for laser intensities $< 2 \times 10^{14}$ W/cm^2 are recorded using a lens of 25 cm focal length, while for the higher laser intensity measurements ($>3 \times 10^{14}$ W/cm^2), a spherical mirror of 3.5 cm focal length was used.

The most striking result at the "low" laser intensity regime ($<2 \times 10^{14}$ W/cm^2) is that the degree of alignment of the Cl^+_{out} angular distributions is almost independent of the laser intensity ($n = 5.0 \pm 0.2 \rightarrow$ fwhm $= 59 \pm 2°$). This result obviously contradicts the predictions of the geometric alignment mechanism according to which an increase of the angular width is definitely anticipated as the laser intensity increases. Therefore, this result implies that the ethyl chloride is dynamically aligned by the laser electric field and also that this procedure is taking place at relatively low laser intensities, within the rise time of the laser pulse, before the electric field reaches the peak intensity. In particular, the alignment procedure is found to take place before the laser intensity reaches the threshold value for double ionization of the ethyl chloride molecule. Since the

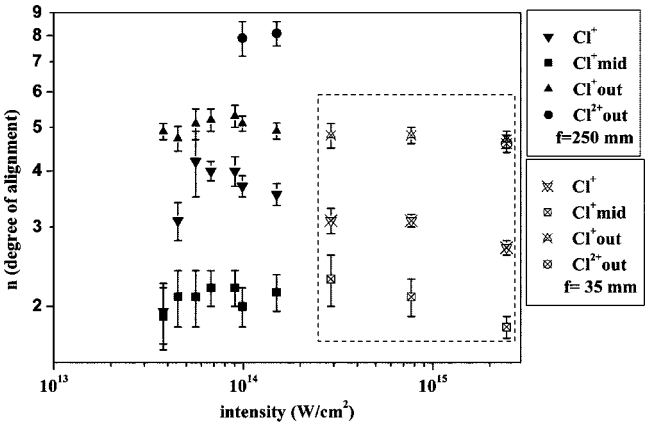

Figure 5. The dependence of the degree of alignment (n) of ethyl chloride fragments on the laser intensity. For laser intensities lower than 2×10^{14} W/cm^2, a $f = 250$ mm lens was used, while for the higher intensity measurements, a spherical mirror ($f = 35$ mm) was employed.

threshold intensity for this molecule is approximately 3×10^{13} W/cm^2, it follows that for a Gaussian laser pulse of 35 ps duration (fwhm) and peak intensity at 10^{14} W/cm^2, the alignment process saturates ~23 ps before the pulse reaches its peak intensity. Thus, although the laser pulse duration is much smaller than the characteristic rotational times of the ethyl chloride, the field-induced alignment takes place unambiguously within the laser pulse, indicating in this way the adiabatic dynamics of the alignment mechanism.

Similar results have been reported for the case of the I_2 and Br_2 molecules under ps laser irradiation at similar laser intensities.[44,45] In particular, Rosca- Pruna et al. reported that for a ~3 ps laser pulse duration, the alignment of the I_2 and Br_2 molecules along the laser electric field takes place mostly at the rise time of the pulse, and therefore, the angular width of the various fragments is independent of the laser peak intensity. However, in order to fully evaluate the alignment mechanism, one needs to investigate the temporal evolution of the alignment during as well as after the end of the laser pulse. Obviously, the single laser pulse technique applied in the present work is not suitable to record the temporal evolution of alignment after the end of the pulse since it induces the photodissociation of the molecular sample, and in that sense, the particular technique is rather limited in comparison to the pump–probe experimental schemes.[14–19]

On the other hand, it could be argued that the observed independence of the degree of alignment on the laser intensity could as well be a consequence of a limited angular resolution of the TOF mass spectrometer. In order to verify that our detection system can be used for high-resolution measurements of angular distributions, we have recorded the angular dependence of N^+ fragments produced by the interaction of molecular nitrogen with 35 ps laser irradiation. The MEDI processes of the particular molecule have been investigated extensively under various laser irradiation conditions in the past. A well-discriminated dissociation channel, consisting of 3.6 ± 0.2 eV kinetic energy fragments, has been observed in the N^+ ion peak of the mass spectra recorded at 2×10^{15} W/cm^2 (not presented here), which is attributed to the dissociation of a doubly charged transient parent ion ($[N_2^{2+}] \rightarrow N^+ + N^+$).[46–48] The degree of alignment of these N^+ fragments (the corresponding angular distribution appears in Figure 4) is found to be $n = 14 \pm 1$ (fwhm $= 35.5 \pm 2°$), which is equivalent to the highest value reported to date for the particular dissociation channel, under similar laser intensities.[10] Hence, the angular resolution of the TOF spectrometer used in the present report is sufficiently high to carry out accurate measurements of angular distributions.

In the present study, the observed independence of the angular width of the $[P^{2+}]$ fragments on the laser peak intensity indicates that the alignment procedure is taking place predominantly before the dissociative ionization of the doubly charged molecular ions $[P^{2+}]$ and that the "postionization alignment"[48] mechanism does not seem to contribute to the final degree of alignment. Since the Cl^+_{out} ions coming from the dissociation of $[P^{2+}]$ are observed at an intensity of $\sim 3 \times 10^{13}$ W/cm^2, the molecular alignment should have been achieved at even lower laser intensities. In other words, the torque exerted on the molecules by the laser field should be strong enough to set the molecules into a pendulum motion within the laser pulse duration at laser intensities lower than $\sim 3 \times 10^{13}$ W/cm^2. Unfortunately, to the best of our knowledge, the polarizability tensors' values for the ethyl chloride molecule are not available in the literature, and as a consequence, the aforementioned conclusion cannot be supported by calculating the molecular rotational motion under the particular laser irradiation conditions.

At the same time, there seems to be a discrepancy between the above result and the recorded dependence of the n parameter on the laser intensity for the entire Cl^+ peak. The "degree of alignment" is found to increase along with the laser intensity, while it reaches a maximum value at a relatively higher value of intensity at $\sim 6.0 \times 10^{13}$ W/cm^2. We believe that the dependence on the laser intensity of the angular distribution of the entire Cl^+ peak cannot be used as a safe criterion for the evaluation of the alignment efficiency since the Cl^+ ion peak includes the contribution of various ionization/dissociation channels ($[P^+]$, $[P^{2+}]$ fragmentation). Therefore, at a particular laser intensity, the characteristics of the Cl^+ angular distribution are expected to depend on the relative strength of the contributing ionization/dissociation channels. The above considerations apply not only to the angular width of the Cl^+ distribution but also to its anisotropy, $(Sign_{Par})/(Sign_{Perp})$.

As mentioned above, the isotropic component of the Cl^+ distribution, that is, the signal recorded with the laser polarization perpendicular to the TOF axis ($Sign_{Perp}$), consists exclusively of low kinetic energy fragment ions, while the Cl^+ ion signal recorded with parallel polarization ($Sign_{Par}$) consists of both low and high kinetic energy fragments. The dependence of the ratios $(Sign_{Par})/(Sign_{Perp})$ and X^+_{out}/X^+_{mid} for $X = Cl^+$ and Cl^{2+} on the laser intensity are presented in Figure 6. Indeed, the dependence of the ratio $(Signal_{Par})/(Sign_{Perp})$ on the laser intensity is similar to that of the n parameter, and therefore, it leads to the same conclusion about the maximum alignment efficiency, which is observed at $\sim 6.0 \times 10^{13}$W/cm^2.

By combining the results of Figures 5 and 6, the conclusion emerges that at low laser intensities ($\sim 4.0 \times 10^{13}$ W/cm^2), the n parameter of the Cl^+ is close to that of the Cl^+_{mid} fragment due to the stronger contribution of these fragments (in comparison to the high kinetic energy ones) to the total ion signal of the Cl^+ peak ($(Cl^+_{out})/(Cl^+_{mid}) < 0.4$). At higher laser intensities of $\sim 6.0 \times 10^{13}$ W/cm^2, the n parameter of the Cl^+ is closer to that of the Cl^+_{out} due to the increased relative contribution of the $[P^{2+}]$ fragmentation ($(Cl^+_{out})/(Cl^+_{mid}) \sim 1.3$). For the same reason, the $(Signal_{Par})/(Sign_{Perp})$ ratio reaches its maximum value at a similar laser intensity value of $(6-7) \times 10^{13}$ W/cm^2. The fact that the fragments of the $[P^{2+}]$ molecular ions are more abundant than the P^+ fragments is clearly a result of the characteristics of the experimental setup, which guarantee that the recorded ionic signal originates from the central portion

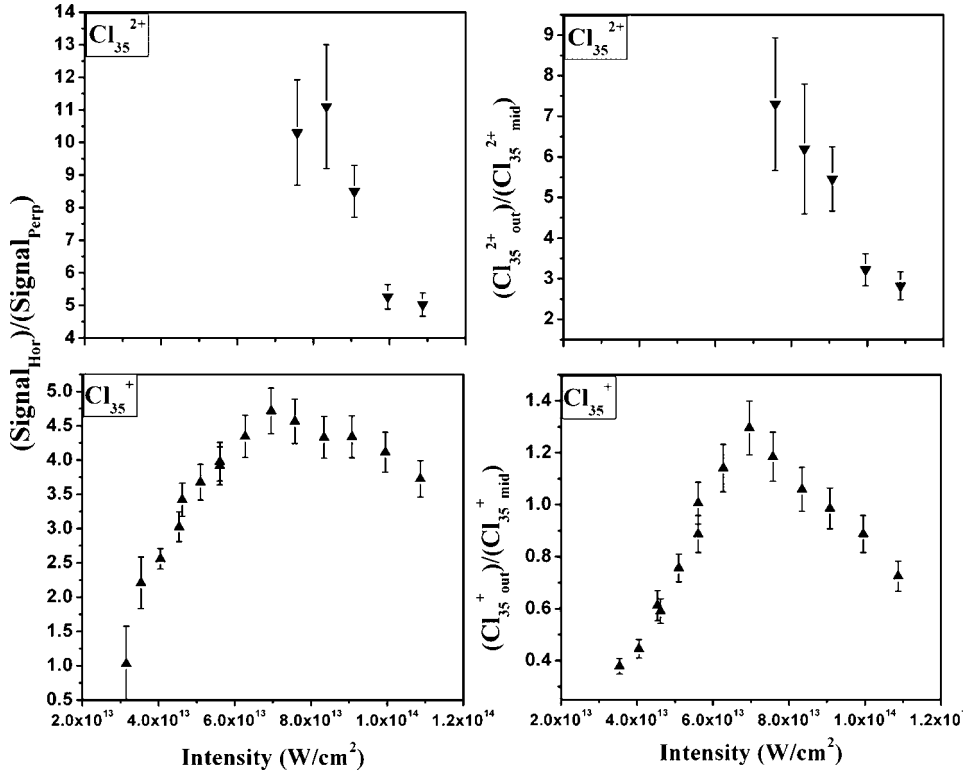

Figure 6. The dependence of the ratios $(Sign_{Par}Cl^{n+})/(Sign_{Perp}Cl^{n+})$ and $Cl^{n+}{}_{out}/\ Cl^{n+}{}_{mid}$, where $n = 1, 2$, on the laser intensity.

of the total focal volume. At even higher laser intensities, a percentage of the $[P^{2+}]$ molecular ions are sequentially ionized to a higher final charge state ($[P^{3+}]$), which leads to the production of Cl^{2+} ions and the reduction of the relative abundance of the $Cl^{+}{}_{out}$ component with respect to the $Cl^{+}{}_{mid}$ one. As the laser intensity is further increased, an equivalent process sets in for the $Cl^{+}{}_{mid}$, which results in the $Cl^{2+}{}_{mid}$ production. This tends to reduce the contribution of the low kinetic energy component $Cl^{+}{}_{mid}$ to the overall Cl^{+} peak. However, at these intensities, the first process leads to the production of doubly charged chloride ions at a higher rate than that of the second one, according to our earlier report.[38] The combination of the processes accounted for above leads to the decreasing values of the ratios $(Cl^{+}{}_{out})/(Cl^{+}{}_{mid})$, $(Cl^{2+}{}_{out})/(Cl^{2+}{}_{mid})$, and $(Signal_{Par})/(Sign_{Perp})$ of the Cl^{+} and Cl^{2+} ions, which are observed at laser intensities higher than $\sim 6.0 \times 10^{13}$ W/cm^2. Therefore, this characteristic laser intensity value should not be related to the maximum alignment efficiency but to the threshold intensity for the generation of the $Cl^{2+}{}_{out}$.

In order to verify the dynamic alignment of the ethyl chloride molecule, the angular distributions of the chloride ions have been recorded at higher laser intensities (3×10^{14} to 2×10^{15} W/cm^2) by focusing the laser beam with a spherical mirror of relatively small focal length ($f = 35$ mm). The interpretation of the experimental results with respect to the alignment mechanism relies on the identification of the various ionization/dissociation channels that contribute to the production of the atomic and molecular fragments. Since there are no reports about the involved processes at such high laser intensities for the molecules under study, we will briefly refer to them in the following paragraph.

In Figure 7, the mass spectra of the ethyl chloride molecule recorded at an intensity of $\sim 2 \times 10^{15}$ W/cm^2 are depicted for laser polarization parallel (solid line) and perpendicular (dash−dot line) to the TOF axis. Multiply charged atomic chloride ions are observed (Cl^{k+}, $k = 1$–4) in the mass spectrum, recorded with parallel laser polarization. These peaks exhibit complex peak profiles that consist of two-pair components, noted as "out" and "mid" in the inset of the figure. The kinetic energies of the Cl^{k+} ions, $k = 1$–3, and the molecular fragment $[P-Cl]^{+}$ are calculated for both components by taking into account the difference in their time-of-flight (Table 1). The kinetic energies of the $Cl^{+}{}_{mid}$ and $Cl^{+}{}_{out}$ are found to be the same, within the range of the experimental errors, as those determined at lower laser intensities ($\sim 10^{14}$ W/cm^2) in our previous report. Thus, the main ionization/dissociation mechanism producing the $Cl^{+}{}_{mid}$ and $Cl^{+}{}_{out}$ components is the dissociation of singly $[P^{+}]$ and doubly $[P^{2+}]$ (channel [1]) charged molecular precursors. As far as the multiply charged ions $Cl^{k+}{}_{out}$ and $Cl^{k+}{}_{mid}$, with $k = 2, 3$, are concerned, their kinetic energies are found to be the same to those of the $Cl^{+}{}_{out}$ and $Cl^{+}{}_{mid}$ ions, respectively. This result indicates that these multiply charged ions are produced by further ionization of the corresponding singly charged ones. Similar results have been reported in the past for the ionization/dissociation processes of alkyl iodides under the same irradiation conditions.[49–51] The validity of the proposed mechanism is also supported by the close resemblance of the angular distributions of all of the $Cl^{k+}{}_{out}$ and $Cl^{k+}{}_{mid}$ components, with $k = 1$–2 (Figure 8).

Hence, this ionization/dissociation mechanism is the dominant one for the $Cl^{2+}{}_{out}$ ions production at $\sim 10^{15}$ W/cm^2, while the contribution of additional dissociation channels can be observed in the peak profile of the $Cl^{2+}{}_{out}$ peak. Indeed, the appearance of the shoulder on either side of the Cl^{2+} peak, noted by an asterisk in Figure 7, indicates the generation of higher kinetic energy fragments ($E_{kin} = 3.9$ eV), which is attributed to the Coulomb explosion of triply charged parent ions (channel [2]), in accordance with that reported previously.[38]

Having clarified the various ionization/dissociation channels leading to the Cl^{+} ions' production, the exploration of the alignment mechanism is feasible. The "degree of alignment" and the corresponding angular width of the $Cl^{+}{}_{out}$ peak recorded

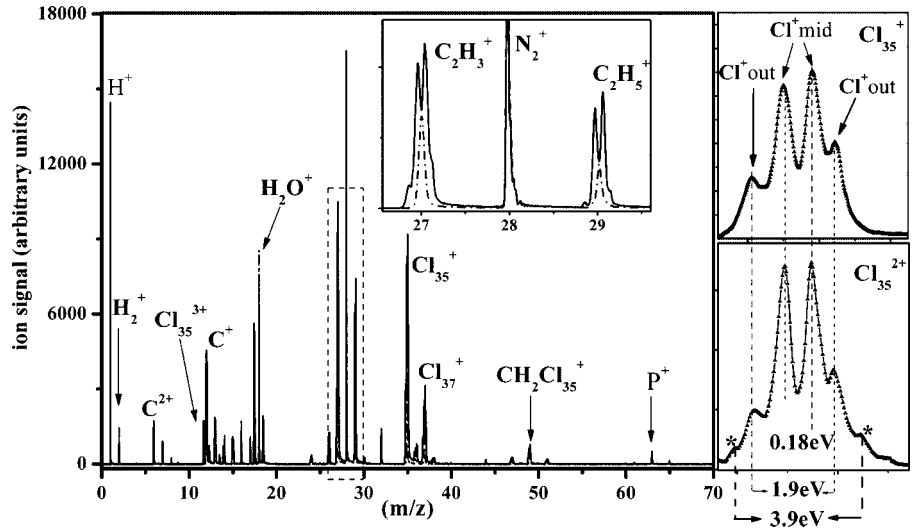

Figure 7. The mass spectra of ethyl chloride recorded at the intensity 10^{15} W/cm^2 for parallel (solid line) and perpendicular (dash−dot line) laser polarization with respect to the TOF axis.

TABLE 1: The Kinetic Energy Values (in eV) of the Ethyl Halide Molecules' Fragment Ions at the Intensity ~10^{15} W/cm^2

	"out" component						"mid" component				
	X^+	X^{2+}	X^{3+}	X^{4+}	X^{5+}	$[P-X]^+$	X^+	X^{2+}	X^{3+}	X^{4+}	$[P-X]^+$
XC_2H_5I	0.72 ± 0.07	0.70 ± 0.07	0.73 ± 0.07	0.76 ± 0.08	0.7 ± 0.1	2.9 ± 0.2	0.08 ± 0.01	0.08 ± 0.01	0.08 ± 0.01		
C_2H_5Br	0.93 ± 0.07	1.1 ± 0.1	1.1 ± 0.1	1.1 ± 0.2		2.7 ± 0.2	0.13 ± 0.03	0.13 ± 0.03	0.14 ± 0.03	0.14 ± 0.03	0.13 ± 0.02
C_2H_5Cl	1.9 ± 0.2	1.8 ± 0.3	1.7 ± 0.3			2.2 ± 0.2	0.22 ± 0.03	0.22 ± 0.03	0.25 ± 0.03		0.24 ± 0.03

at an intensity of 1.7×10^{15} W/cm^2 is found to be $n = 4.7 \pm 0.1$. Thus, the corresponding angular width (fwhm = 61 ± 2°) is the same, within the range of experimental errors, as that recorded at much lower laser intensities (for example, 59 ± 2° at 6×10^{13} W/cm^2), proving unambiguously that the ethyl chloride molecule is dynamically aligned by the laser field. On the contrary, for the case of the Cl^{2+}_{out} component, the "degree of alignment" is drastically reduced as the laser intensity increases from 10^{14} W/cm^2 ($n = 8.0 \pm 0.7$, fwhm = 47 ± 3°) to 1.7×10^{15} W/cm^2 ($n = 4.7 \pm 0.2$, fwhm = 61 ± 2°). Although such an observation is usually considered as an indication of the geometric alignment mechanism, in the present case, the broadening of the Cl^{2+}_{out} component is attributed to the enhanced contribution of the double ionization of atomic chloride ions Cl^+_{out} released from the coulomb explosion of the $[P^{2+}]$ precursors.

Finally, serving the thoroughness of the investigation of the alignment mechanism, we have compared the ionic signals produced for linear and circular laser polarization. According to theoretical models[52–55] and related experimental reports[56,57] concerning the enhanced molecular ionization phenomenon, the ionization rate is mainly dependent on the laser electric field component parallel to the axis of maximum molecular polarization, provided that the ionization is a field ionization process. In the case of ethyl chloride, the axis of maximum polarization is expected to be close to the C−Cl molecular bond direction.[58] For circular polarization, the laser electric field rotates too quickly for any molecule to follow, and therefore, the produced ion signal is expected to be spherically symmetric in the plane of the electric field rotation. Thus, by retaining a small acceptance angle for the TOF spectrometer and the same laser electric field component along the detection axis, the comparison of the ionic signal recorded for linear and circular polarization can be used for the evaluation of the alignment mechanism (dynamic vs geometric alignment).[59]

The signal of the Cl^+_{out}, Cl^{2+}_{out}, and $[P-Cl]^+_{out}$ ionic fragments recorded for linear (dash-dot line) and circular polarization (dotted line) at the intensity of 7.5×10^{14} and 1.5×10^{15} W/cm^2, respectively, is presented in Figure 9. The comparison is based on the assumption that the dominant ionization mechanism is the field ionization one. At an intensity of 7.5×10^{14} W/cm^2, the Keldysh parameter [$\gamma = (IP/Up)^{1/2}$, where IP is the ionization potential and Up is the ponderomotive potential of the free electron] is smaller than one ($\gamma \sim 0.37$), implying that the ionization of ethyl chloride should proceed through a field ionization process.[60] However, for the case of polyatomic molecules, it is known that the Keldysh parameter is not a safe criterion for the discrimination of the field ionization and MP ionization regimes since the contribution of MPI processes has been identified for irradiation conditions such that $\gamma \ll 1$.[61] Moreover, the contribution of MPI processes cannot be excluded especially in the spatial and temporal wings of the intensity distribution of the focused laser beam. The particular fragments Cl^+_{out}, Cl^{2+}_{out}, and $[P-Cl]^+_{out}$ have been chosen for the evaluation of the alignment mechanism because they are produced at least partly from the direct dissociation of multiply charged molecular ions and also due to their high kinetic energy, which guarantees a good angular resolution of the TOF spectrometer. The ionic signal of the aforementioned peaks recorded with linear laser polarization is clearly stronger than the corresponding with circular polarization. The ionic signal for the Cl^+_{out} and Cl^{2+}_{out} fragments for linear polarization is, for both cases, about 1.8 times higher than that recorded with circular polarization. The observed difference is unambiguous and can be considered as a strong indication of the dynamic alignment of the ethyl chloride molecules with respect to the laser electric field.

The Ethyl Bromide and Ethyl Iodide Cases. The analysis of the experimental data recorded at the high laser intensity range (~10^{15} W/cm^2) indicates that the ionization/dissociation processes for ethyl bromide and ethyl iodide are similar to those identified for the ethyl chloride. The kinetic energies of the X^+ and $[P-X]^+$ fragments for both components ("out" and "mid"), which are presented in Table 1, are found to be the same as the

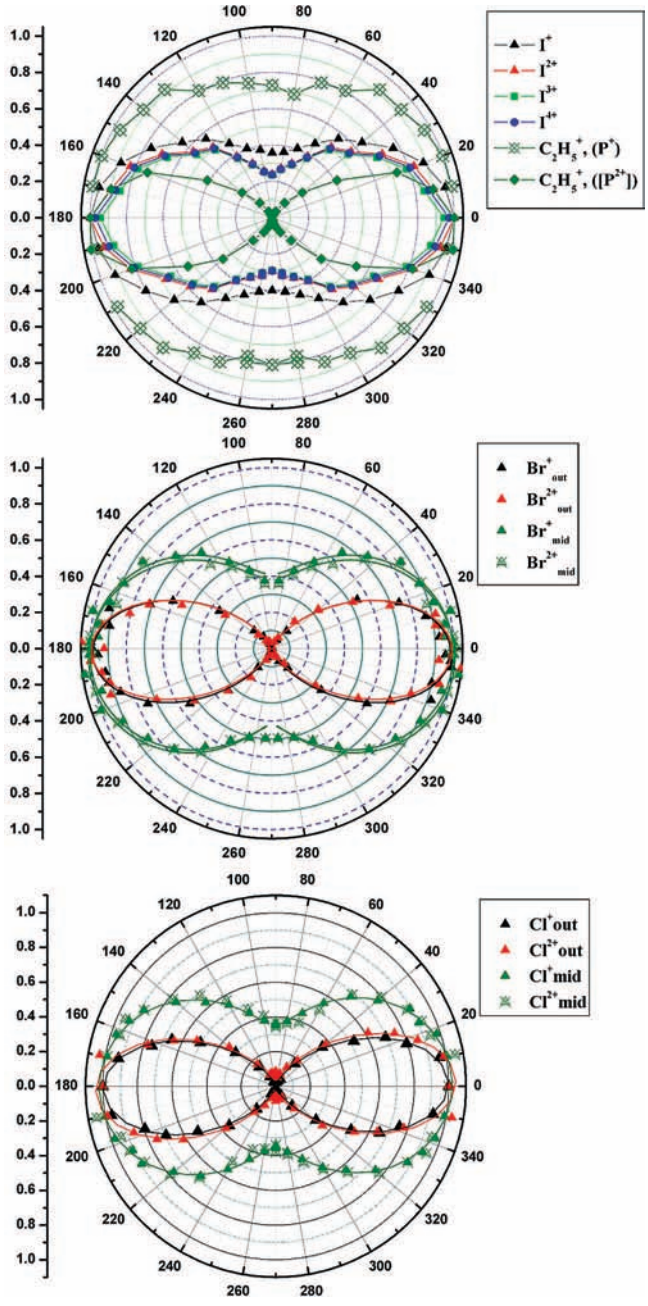

Figure 8. The angular distributions of the ethyl halide molecules' fragments at the intensity $\sim 10^{15}$ W/cm^2.

corresponding values at a lower laser intensity of $\sim 10^{14}$ W/cm^2.[38] Thus, in agreement with that reported earlier, the X^+_{out} and $[P-X]^+_{out}$ ions are ejected by the Coulomb explosion of the $[P^{2+}]$ parent ions, while the corresponding "mid" components are generated by the dissociation of singly charged parent ions. The kinetic energy values of the multiply charged halogen ions (X^{k+}, $k = 2$–4) are found to be the same for both components as those of the singly charged halogen ions. Therefore, the major part of the ionic signal of the multiply charged halogen ions should be attributed to the further ionization of the singly charged ones released by the two aforementioned ionization/dissociation channels, while both processes are taking place within the laser pulse duration. For the ethyl bromide, the proposed mechanism is also supported by the common angular distributions of the Br^{n+}_{out} and Br^{n+}_{mid} ions with $n = 1$–2 (Figure 8). Moreover, an additional dissociation channel contributing to the abundance of the ≪out≫ components of the X^{2+} ions for both the ethyl bromide and ethyl iodide molecules has been confirmed in our previous report, namely, the Coulomb explosion of triply charged parent ions.

As far as the alignment mechanism of the ethyl bromide and ethyl iodide molecules is concerned, the corresponding experimental results are also found to be in accordance with the ones presented for ethyl chloride. Especially for the case of ethyl bromide, the angular width of the $[P^{2+}]$ fragments' distribution is found to be independent of the laser intensity (fwhm $= 66 \pm 3°$) for a wide range of values (3×10^{13} to 2×10^{15} W/cm2). For the ethyl iodide molecule, the various ionization/dissociation channels can be safely discriminated in the peak profile of the $[P-I]^+$ molecular fragment. In this case, the angular distributions of the $[P-I]^+_{out}$ components coming from the Coulomb explosion of the $[P^{2+}]$ precursors have approximately the same angular width (fwhm $= 60 \pm 3°$) for laser intensities in the range of 3×10^{13} to 2×10^{15} W/cm^2. Thus, in agreement with the experimental results for the ethyl chloride, the dynamic alignment of the ethyl bromide and ethyl iodide molecules is found to take place at relatively low laser intensity ($<3 \times 10^{13}$ W/cm^2) at the rise time of the laser pulse, that is, below the intensity threshold for the double ionization of the molecules under study. In addition, the dynamic alignment of these molecules has been confirmed by using the criterion based on the comparison of the ionic signals recorded with linear and circular polarization (data not presented here).

Especially for the case of the ethyl iodide, rough calculations of its rotational motion, under laser irradiation, can be performed by using the equation:

$$\frac{d^2\theta}{dt^2} = -\frac{(a_{\parallel} - a_{\perp})}{4I(t)} E_o^2(t) \sin(2\theta)$$

where θ is the angle between the C−I bond and the E electric field, I is the moment of inertia, and $a_{\parallel} - a_{\perp}$ is the anisotropy of the molecular polarizability.[11,13,45] The values of the ethyl iodide polarizability tensors have been reported recently.[62] The calculations were performed by treating the molecule as a symmetric top rigid rotor since the rotational constants with respect to axes normal to the C−I molecular bond are roughly the same ($B = 2979.566$ MHz; $C = 2796.451$ MHz). Moreover, the temporal profile of the laser pulse is considered to be a Gaussian with a fwhm of 35 ps. Under these assumptions and for a laser peak intensity of 10^{14} W/cm^2, it has been found that ethyl iodide is forced into a pendular motion with respect to the laser field before the laser peak intensity is reached. Actually, for a rotationally cold molecular ensemble, the molecules are trapped in a pendular motion when the laser field reaches a value of $\sim 7 \times 10^{11}$ W/cm^2, while for the case of rotating molecules at room temperature (300 K), the corresponding laser field is $\sim 7 \times 10^{12}$ W/cm^2. These values are obviously much lower than the intensity needed to achieve the double ionization of the ethyl iodide, in agreement with the conclusions drawn on the basis of the experimental results. Therefore, the alignment of the ethyl iodide during its interaction with 35 ps laser pulses takes place within the rise time of the laser pulse, and the overall procedure is close to the adiabatic limit, even though the duration of the pulse is approximately one-fifth of the characteristic rotational time ($1/2B$ (Hz)).

Comparison of the Alignment Efficiency of the Ethyl Halide Molecules. Having proven the dynamic alignment of these molecules, it is reasonable to go a step further and compare their alignment efficiency. The comparison of the alignment efficiency of the ethyl bromide and ethyl chloride molecules is based on the comparison of the angular distribution width of

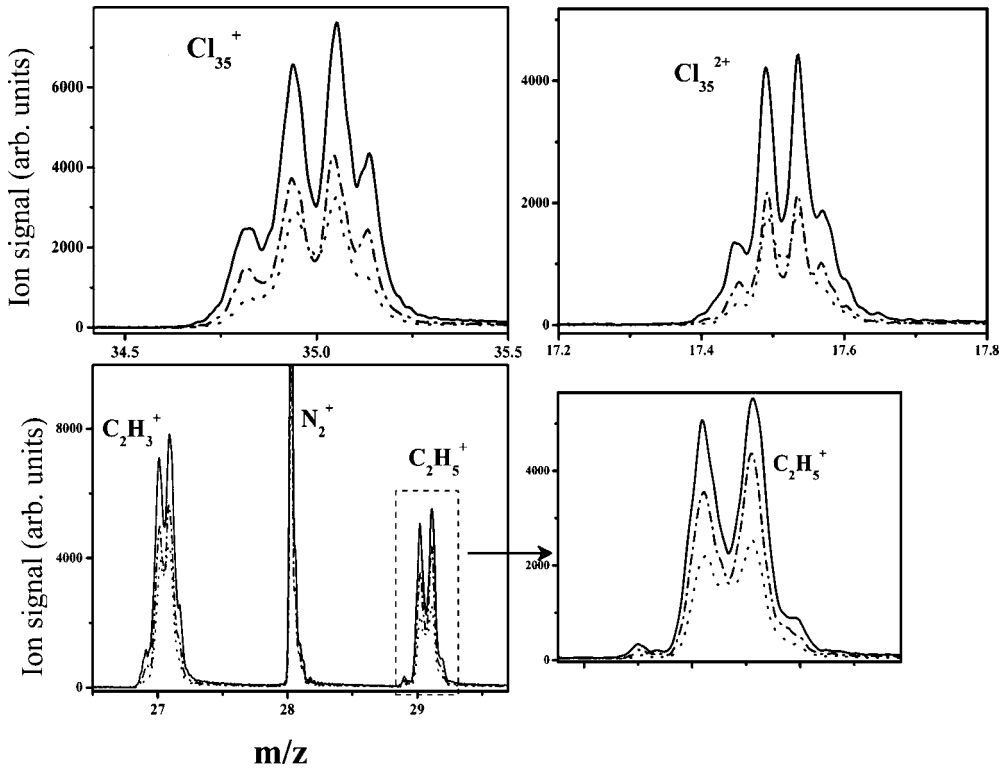

Figure 9. The ionic signal of ethyl chloride fragments recorded for linear polarization at the intensity 1.5×10^{15} W/cm^2 (solid line) and 7.5×10^{14} W/cm^2 (dash−dot line) in comparison to that recorded for circular polarization at 1.5×10^{15} W/cm^2 (dot line).

TABLE 2: The FWHM of the Ethyl Halide Fragments' Angular Distributions Recorded at $\sim 1 \times 10^{14}$ W/cm^2, $\lambda = 1064$ nm, and $\tau = 35$ ps ("mid" and "out" components correspond to singly and multiply charged molecular precursors)

		$\sum_{y=1-5} C_2H_y^+$ *mid*	$\sum_{y=1-5} C_2H_y^+$ *out*	X^+_{out}	X^+_{mid}	X^{2+}_{out}
fwhm (°)	I	105 ± 4	65 ± 3			
	Br	105 ± 4	66 ± 3	66 ± 3	102 ± 5	51 ± 2
	Cl	92 ± 4	59 ± 2	59 ± 2	90 ± 3	47 ± 2

the "out" components of the X^+, X^{2+} ions recorded at the same laser intensity of $\sim 10^{14}$ W/cm^2. At this laser intensity, the X^{2+}_{out} ions are generated via Coulomb explosion within triply charged transient parent ions as it is verified by the estimated higher kinetic energy values for these species. The Coulomb explosion fragments are chosen due to their high kinetic energy values, which ensure that the angular resolution of the TOF mass spectrometer is sufficient enough to perform accurate angular distribution measurements. Moreover, we choose to compare the angular widths at relatively low laser intensity, where the X^+_{out} and X^{2+}_{out} ions are produced mainly by the direct dissociation of $[P^{2+}]$ and $[P^{3+}]$ molecular precursors, respectively.

For the case of the ethyl iodide molecule, the "out" components cannot be safely resolved in the peak profiles of the I^+ and I^{2+} ions. Nevertheless, the alignment efficiency for the $[P^{2+}]$ precursors could be measured, indirectly, by the angular distribution of the $[P-I]^+_{out}$ peak components. Instead of this particular peak, we are using the angular distribution of the sum of the $C_2H_y^+$ ($y = 1$–5) fragments in order to take into account all of the possible dissociation channels of the $[P^{2+}]$ precursors. Apart from the fragmentation of the C−I bond, the I^+ ions can also be produced by dissociation channels, which include the simultaneous cleavage of C−H bonds and the elimination of H or H_2 fragments. The same is also valid for the corresponding ethyl bromide and chloride molecules according to some earlier reports.[38,63] This particular choice is justified for the case of the ethyl bromide and ethyl chloride molecules by the angular distributions of the

$$\sum_{y=1}^{5} C_2H_y^+ \quad mid$$

and

$$\sum_{y=1}^{5} C_2H_y^+ \quad out$$

ions, respectively, while for the ethyl iodide, the same conclusion is supported by the similarity of the angular distributions of the

$$\sum_{y=1}^{5} C_2H_y^+$$

and

$$\sum_{y=1}^{3} I^{n+}$$

sums. The fwhm of the various fragment distributions are presented in Table 2. Since the X^+_{out} and X^{2+}_{out} ions, presented in this Table 2, are products of Coulomb explosion taking place within multiply charged parent ions, the fwhm of their angular distributions is not identical anymore (as in Figure 8). The leading precursors in X^{2+}_{out} ion production are species with a

TABLE 3: The Values of the Moment of Inertia for the Ethyl Halide Molecules under Study[63]

	moment of inertia (amu Å^2)		
	I_C	I_β	I_A
C_2H_5I	180.72	169.61	17.35
C_2H_5Br	133.338	142.98	16.281
C_2H_5Cl	99.468	90.244	15.886

higher degree of alignment (dependence of the ionization probability on the alignment with respect to the laser field) and therefore present sharper angular distributions. It is interesting to note that the trend of the fwhm of the angular distributions for the $X^{2+}{}_{out}$ fragments follows that of the $X^{+}{}_{out}$ ions.

The angular widths of the C_2H_5I and C_2H_5Br distributions are found to be the same within the range of the experimental error. On the other hand, the fwhm of the C_2H_5Cl distributions for the singly and doubly charged fragments are about 11−12% smaller than the corresponding ones for the heavier molecules. The similarity of the alignment efficiency of the molecules under study is somewhat impressive considering the fact that the masses of the halogen atoms (I/Br/Cl = 127/81−79/37−35) and the moments of inertia of the corresponding molecules (Table 3) are largely different. This result is at variance with several earlier reports on the alignment of small molecules by strong laser fields of fs duration. For the case of relatively light molecules, such as H_2 and N_2, the dynamic alignment is achievable with laser pulses of 50 fs duration, while this is impossible for heavier molecules, such as I_2, where the dominant alignment mechanism is found to be the geometric one.[10] Furthermore, Ellert et al.[13] concluded that the degree of alignment of some diatomic molecules (Cl_2, Br_2, O_2, and I_2) under laser irradiation of 80 fs pulse duration is decreasing for increasing moments of inertia. On the contrary, for a pulse duration long enough to restrict the molecular systems in pendular states, the alignment efficiency may even be increased for heavier molecules, according to theoretical predictions[22,23] and recent experimental results with slightly longer laser pulses.[64]

In the present case, our experimental findings are clearly at variance with those reported for short pulse durations, as a result of the 35 ps duration which is proven to be long enough to induce the dynamic alignment of all of the studied molecules at the rise time of the laser pulse and prior to their double ionization, despite their largely different moments of inertia.

A plausible interpretation emerges from the classical equation describing the laser-induced molecular rotation, according to which the rotational acceleration and, therefore, the time required for efficient reorientation depend on the ratio of the anisotropy of the molecular polarizability to the moment of inertia. Taking into account that the polarizability of the C−X bond increases from Cl to Br to I, it is expected that the anisotropy of molecular polarizability should follow the same trend for the ethyl halide molecules. Thus, it could be argued that the similar alignment efficiency of the particular molecules could be attributed to their similar angular acceleration under the same laser irradiation conditions.

At the same time, it is known that another important parameter determining the alignment efficiency is the maximum laser intensity which the molecules can withstand prior to their dissociative ionization.[22,23,64] Therefore, by taking into account that the laser intensities required for single and multiple molecular ionization of the ethyl halides increase as the halogen mass decreases (from I to Br to Cl), the observed similarity in the alignment efficiency can also be considered unexpected. However, this argument can by no means lead to a conclusion on whether the alignment takes place before or/and after the single molecular ionization since the comparison of the alignment efficiency is based on the degree of alignment of the $[P^{2+}]$ fragments. Hence, the comparison reflects the total degree of alignment, namely, the overall contribution of the alignment processes, taking place before (alignment of neutral molecules) and after the single molecular ionization (alignment of ions).

Conclusions

The ejection anisotropy in the Coulomb explosion of some ethyl halide molecules, under strong ps laser irradiation, is investigated by means of time-of-flight mass spectrometry. The molecules (C_2H_5X, where X = I, Br, Cl) were irradiated at 1064 nm, while the 35 ps laser intensity was in the range of 2×10^{13} to 2×10^{15} W/cm^2.

The angular distributions of the Coulomb explosion halogen fragment ions are indicative of the dynamic alignment of the corresponding multiply charged precursors. The alignment mechanism has been verified by recording the dependence of their angular distribution characteristics on the laser intensity. In particular, the angular width of the X^+ and $[P-X]^+$ ion distributions, originating from transient doubly charged parent ions, was found to be independent of the laser intensity. This result obviously contradicts the predictions of the geometric alignment mechanism, according to which an increase of the angular width is definitely anticipated as the laser intensity increases. Therefore, it is concluded that the molecules under study are dynamically aligned by the laser electric field and, also, that this process is taking place within the rise time of the laser pulse, at lower laser intensities than those required for the multiple molecular ionization. The same conclusion is supported for the ethyl iodide case by solving numerically the classical equation describing the molecular rotational motion under laser irradiation. The dynamic alignment of the ethyl halides has also been confirmed by comparing the abundance of the fragment ions for linearly and circularly polarized laser irradiation with equal electric field components along the TOF axis.

From the comparative analysis of the experimental results, it is concluded that the characteristics of the angular distributions (angular width, ratio of its maximum value to the minimum one) of the entire X^+ and X^{2+} ion peaks are determined by the relative strength of the contributing ionization/dissociation channels, and therefore, their dependence on the laser intensity cannot be used as a safe criterion for the identification of the alignment mechanism.

Finally, from the comparison of the angular distributions widths of the Coulomb explosion fragment ions, it is concluded that the degree of alignment is only weakly dependent on the mass of the halogen atom and the molecular moment of inertia.

Acknowledgment. We would like to express our thanks to the Central Laser Facility of the University of Ioannina for their facilities and their assistance. This research was funded by the program "Heraklitos" of the Operational Program for Education and Initial Vocational Training of the Hellenic Ministry of Education under the third Community Support Framework and the European Social Fund.

References and Notes

(1) Normand, D.; Lompre, L. A.; Cornaggia, C. *J. Phys. B: At. Mol. Opt. Phys.* **1992**, *25*, L497.
(2) Dietrich, P.; Strickland, D. T.; Laberge, M.; Corkum, P. B. *Phys. Rev. A* **1993**, *47*, 2305.
(3) Minemoto, S.; Tanji, H.; Sakai, H. *J. Chem. Phys.* **2003**, *119*, 7737.

(4) Minemoto, S.; Sakai, H. *Phys. Rev. A* **2007**, *75*, 33413.
(5) Voss, S.; Alnaser, A. S.; Tong, X.-M.; Maharjan, C.; Ranitovic, P.; Ulrich, B.; Shan, B.; Chang, Z.; Lin, C. D.; Cocke, C. L. *J. Phys. B: At. Mol. Opt. Phys.* **2004**, *37*, 4239.
(6) Graham, P.; Ledingham, K. W. D.; Singhal, R. P.; McCanny, T.; Hankin, S. M.; Fang, X.; Tzallas, P.; Kosmidis, C.; Taday, P. F.; Langley, A. J. *J. Phys. B: At. Mol. Opt. Phys.* **2000**, *33*, 3779.
(7) Graham, P.; Fang, X.; Ledingham, K. W. D.; Ledingham, K. W. D.; Smith, D. J.; Kosmidis, C.; Tzallas, P.; Langley, A. J.; Taday, P. F. *Laser Part Beams* **2000**, *18*, 417.
(8) Kumar, G. R.; Gross, P.; Safvan, C. P.; Rajgara, F. A.; Mathur, D. *Phys. Rev. A* **1996**, *53*, 3098.
(9) Rost, J. M.; Griffen, J. C.; Friedrich, B.; Herschbach, D. R. *Phys. Rev. Lett.* **1992**, *68*, 1299.
(10) Posthumus, J. H.; Plumridge, J.; Thomas, M. K.; Codling, K.; Frasinski, L. J.; Langley, A. J.; Taday, P. F. *J. Phys. B: At. Mol. Opt. Phys.* **1998**, *31*, L553.
(11) Banerjee, S.; Kumar, G. R.; Mathur, D. *Phys. Rev. A* **1999**, *60*, R3369.
(12) Rajgara, F. A.; Mathur, D.; Ramachandran, H. *Chem. Phys. Lett.* **2007**, *438*, 31.
(13) Ellert, Ch.; Corkum, P. B. *Phys. Rev. A* **1999**, *59*, R3170.
(14) Sakai, H.; Safvan, C. P.; Larsen, J. J.; Hilligsoe, K. M.; Hald, K.; Stapelfeldt, H. *J. Chem. Phys.* **1999**, *110*, 10235.
(15) Larsen, J. J.; Sakai, H.; Safvan, C. P.; Larsen, I. W.; Stapelfeldt, H. *J. Chem. Phys.* **1999**, *111*, 7774.
(16) Underwood, J. G.; Spanner, M.; Ivanov, M. Y.; Mottershead, J.; Sussman, J.; Stolow, A. *Phys. Rev. Lett.* **2003**, *90*, 223001.
(17) Renard, V.; Renard, M.; Guerin, S.; Pashayan, Y. T.; Lavorel, B.; Faucher, O.; Jauslin, H. R. *Phys. Rev. Lett.* **2003**, *90*, 153601.
(18) Comstock, M.; Senekerimyan, V.; Dantus, M. *J. Phys. Chem. A* **2003**, *107*, 8271.
(19) (a) Kim, W.; Felker, P. M. *J. Chem. Phys.* **1996**, *104*, 1147. (b) Kim, W.; Felker, P. M. *J. Chem. Phys.* **1997**, *107*, 2193. (c) Kim, W.; Felker, P. M. *J. Chem. Phys.* **1998**, *108*, 6763. (d) Kim, W.; Schaeffer, M. W.; Lee, S.; Chung, J. S.; Felker, P. M. *J. Chem. Phys.* **1999**, *110*, 11264.
(20) (a) Rosca-Pruna, F.; Vrakking, M. J. J. *J. Chem. Phys.* **2002**, *116*, 6567. (b) Rosca-Pruna, F.; Vrakking, M. J. J. *J. Chem. Phys.* **2002**, *116*, 6579.
(21) Rosca-Pruna, F.; Vrakking, M. J. J. *Phys. Rev. Lett.* **2001**, *87*, 153902.
(22) Seideman, T.; Hamilton, E. *Adv. At., Mol., Opt. Phys.* **2006**, *52*, 289.
(23) Stapelfeldt, H.; Seideman, T. *Rev. Mod. Phys.* **2003**, *75*, 543.
(24) Loriot, V.; Tzallas, P.; Benis, E. P.; Hertz, E.; Lavorel, B.; Charalambidis, D.; Faucher, O. *J. Phys. B: At. Mol. Opt. Phys.* **2007**, *40*, 2503.
(25) Torres, R.; Kajumba, N.; Underwood, J. G.; Robinson, J. S.; Baker, S.; Tisch, J. W.; de Nalda, R.; Bryan, W. A.; Velotta, R.; Altucci, C.; Turcu, I. C.; Marangos, J. P. *Phys. Rev. Lett.* **2007**, *98*, 203007.
(26) LéPine, F.; Kling, M. F.; Ni, Y. F.; Khan, J.; Ghafur, O.; Martchenko, T.; Gustafsson, E.; Johnsson, P.; Varjú, K.; Remetter, T.; L'huillier, T.; Vrakking, M. J. J. *J. Mod. Opt.* **2007**, *54*, 953.
(27) Hertz, E.; Rouzée, A.; Guérin, S.; Lavorel, B.; Faucher, O. *Phys. Rev. A* **2007**, *75*, 31403.
(28) Pinkham, D.; Mooney, K. E.; Jones, R. R. *Phys. Rev. A* **2007**, *75*, 13422.
(29) Bryan, W. A.; English, E. M. L.; Mc Kenna, J.; Wood, J.; Calvert, C. R.; Turku, I. C. E.; Torres, R.; Collier, J. L.; Williams, J. D.; Nevel, W. R. *Phys. Rev. A* **2007**, *76*, 23414.
(30) Holmegaard, L.; Viftrup, S. S.; Kumarappan, V.; Bisgaard, C. Z.; Stapelfeldt, H.; Hamilton, E.; Seideman, T. *Phys. Rev. A* **2007**, *75*, 051403.
(31) Kumarappan, V.; Viftrup, S. S.; Holmegaard, L.; Bisgaard, C. Z.; Stapelfeldt, H. *Phys. Scr.* **2007**, *76*, C63.
(32) Lee, K.F.; Villeneuve, D. M.; Corkum, P. B.; Stolow, A.; Underwood, J. G. *Phys. Rev. Lett.* **2006**, *97*, 173001.
(33) Poulsen, M. D.; Ejdrup, T.; Stapelfeldt, H.; Hamilton, E.; Seideman, T. *Phys. Rev. A* **2006**, *73*, 033405.
(34) Poulsen, M.D.; Péronne, E.; Stapelfeldt, H.; Bisgaard, C. Z.; Viftrup, S. S.; Hamilton, E.; Seideman, T. *J. Chem. Phys.* **2004**, *121*, 783.
(35) Ortigoso, J.; Rodrıguez, M.; Gupta, M.; Friedrich, B. *J. Chem. Phys.* **1999**, *110*, 3870.
(36) Cai, L.; Friedrich, B. *Collect. Czech. Chem. Commun.* **2001**, *66*, 991.
(37) Torres, R.; de Nalda, R.; Marangos, J. P. *Phys. Rev. A* **2005**, *72*, 023420.
(38) Kaziannis, S.; Kosmidis, C. *J. Phys. Chem. A* **2007**, *111*, 2839.
(39) August, S.; Meyerhofer, D.; Strickland, D.; Chin, S. L. *J. Opt. Soc. Am. B* **1991**, *8*, 858.
(40) Litvinyuk, I. V.; Lee, K. F.; Dooley, P. W.; Rayner, D. M.; Villeneuve, D. M.; Corkum, P. B. *Phys. Rev. Lett.* **2003**, *90*, 233003.
(41) Pavicic, D.; Lee, K. F.; Rayner, D. M.; Corkum, P. B.; Villeneuve, D. M. *Phys. Rev. Lett.* **2007**, *98*, 243001.
(42) Pinkham, D.; Jones, R. R. *Phys. Rev. A* **2005**, *72*, 023418.
(43) Schmidt, M.; Dobosz, S.; Meynadier, P.; D'Oliveira, P.; Normand, D.; Charron, E.; Suzor-Weiner, A. *Phys.Rev. A* **1999**, *60*, 4706.
(44) Rosca-Pruna, F.; Springate, E.; Offerhaus, H. L.; Krishnamurthy, M.; Farid, N.; Nicole, C.; Vrakking, M. J. J. *J. Phys. B: At. Mol. Opt. Phys.* **2001**, *34*, 4919.
(45) Springate, E.; Rosca-Pruna, F.; Offerhaus, H. L.; Krishnamurthy, M.; Vrakking, M. J. J. *J. Phys. B: At. Mol. Opt. Phys.* **2001**, *34*, 4939.
(46) Tong, X. M.; Zhao, Z. X.; Alnaser, A. S.; Voss, S.; Cocke, C. L.; Lin, C. D. *J. Phys. B: At. Mol. Opt. Phys.* **2005**, *38*, 333.
(47) Cornaggia, C.; Lavancier, J.; Normand, D.; Morellec, J.; Angostini, P.; Chamborent, J. P.; Antonetti, A. *Phys. Rev. A* **1991**, *44*, 4499.
(48) Lavancier, J.; Normand, D.; Cornaggia, C.; Morellec, J.; Liu, H. X. *Phys. Rev. A* **1991**, *43*, 1461.
(49) Siozos, P.; Kaziannis, S.; Kosmidis, C. *Int. J. Mass. Spectrom.* **2003**, *225*, 249.
(50) Siozos, P.; Kaziannis, S.; Kosmidis, C.; Lyras, A. *Int. J. Mass. Spectrom.* **2005**, *243*, 189.
(51) Kaziannis, S.; Siozos, P.; Kosmidis, C. *Chem. Phys. Lett.* **2005**, *401*, 115.
(52) Frasinski, L. J.; Codling, K.; Hatherly, P. A.; Barr, J. R.; Ross, R. N.; Toner, W. T. *Phys. Rev. Lett.* **1987**, *58*, 2424.
(53) Posthumus, J. H.; Frasinski, L. J.; Giles, A. J.; Codling, K. *J. Phys. B: Atom. Mol. Opt. Phys.* **1995**, *28*, L349.
(54) Seideman, T.; Yvanov, M. Yu.; Corkum, P. B. *Phys. Rev. Lett.* **1995**, *75*, 2819.
(55) Chelkowski, S.; Bandrauk, A. D. *J. Phys. B: Atom. Mol. Opt. Phys.* **1995**, *28*, L723.
(56) Constant, E.; Stapelfeldt, H.; Corkum, P. B. *Phys. Rev. Lett.* **1996**, *76*, 4140.
(57) Posthumus, J. H. *Rep. Prog. Phys.* **2004**, *67*, 623.
(58) Castillejo, M.; Martın, M.; Nalda, R.; Couris, S.; Koudoumas, E. *J. Phys. Chem. A* **2002**, *106*, 2838.
(59) Ellert, C.; Corkum, P. B. *Phys. Rev. A* **1999**, *59*, R3170.
(60) Keldysh, L. V. *Sov. Phys. JEPT* **1965**, *20*, 1307.
(61) Kosmidis, C.; Siozos, P.; Kaziannis, S.; Robson, L.; Ledingham, K. W. D.; McKenna, P.; Jaroszynski, D. A. *J. Phys. Chem. A* **2005**, *109*, 1279.
(62) Poulsen, M. D. Ph.D. Thesis, Department of Chemistry, University of Aarhus, Denmark, 2005, p 152.
(63) NIST Chemistry WebBookWeb Page. http://webbook.nist.gov.
(64) Zhao, K.; Hill, W. T., III *Phys. Rev. A* **2005**, *71*, 013412.

JP710540R